Journal of Solid Mechanics Vol. 5, No. 3 (2013) pp. 278-289

Analytical Prediction of Indentation and Low-Velocity Impact Responses of Fully Backed Composite Sandwich Plates

M. Hosseini[1], S.M.R. Khalili[1,2,*]

[1]*Centre of Excellence for Research in Advanced Materials and Structures, Faculty of Mechanical Engineering, K.N. Toosi University of Technology, Tehran, Iran*
[2]*Faculty of Engineering, Kingston University, London, UK*

Received 12 June 2013; accepted 2 August 2013

ABSTRACT

In this paper, static indentation and low velocity impact responses of a fully backed composite sandwich plate subjected to a rigid flat-ended cylindrical indenter/impactor are analytically investigated. The analysis is nonlinear due to nonlinear strain-displacement relation. In contrast to the existed analytical models for the indentation of composite sandwich plates, the stacking sequence of the face sheets can be completely arbitrary in the present model. Furthermore, the effects of the initial in-plane normal and shear forces on the edges of the sandwich plate are also considered. Based on these modifications, an improved contact law (contact force – indentation relation) is derived. The low velocity impact analysis of the problem is performed using a discrete system of spring-mass-dashpot model. The characteristics of the equivalent spring and dashpot are identified from the derived contact law and by incorporating the effect of the dynamic material properties of the sandwich plate. Analytical predictions of the load-indentation response as well as the impact force history are compared well with the experimental results in the literature. The effects of various parameters on both indentation and impact responses of the sandwich plates are qualitatively and quantitatively investigated.

Keywords: Indentation; Low velocity impact; Composite sandwich plate

1 INTRODUCTION

STRUCTURAL composite sandwich panels with the composite face sheets are nowadays widely used in aerospace, automobile, locomotive, windmills, buildings, and consumer industries for their excellent properties. However, to use them securely and effectively under various loading conditions, their mechanical behavior should be well understood and known. During service, these panels may encounter low velocity impacts caused by runway stones, hails, tool drop, tire blowout debris, etc. Although, extensive research has been devoted to the impact behavior of composite laminates in general [1-5], the work on sandwich structures is somewhat limited. In this context, the work of Williamson and Lagace [6] may be mentioned in which some experiments were performed to study the static indentation and impact behavior of composite sandwich plates. They gauged the face sheet deflection under the indenter and also studied the core and the face sheet damages with varying core thickness and laminate lay-up. They found that the load-deflection characteristics and failure predictions of the sandwich plates under static indentation and low velocity impact tests were similar.

* Corresponding author. Tel.: +98 2188674747; Fax: +98 2188674748.
E-mail address: smrkhalili2005@gmail.com (S.M.R. Khalili).

Herup and Palazotto [7] performed the low-velocity impact and static indentation tests on sandwich plates composed of 4 to 48-plies graphite/epoxy cross-ply laminate face sheets and Nomex honeycomb cores to characterize the damage initiation as a function of face sheet thickness and loading rate. Turk and Hoo Fatt [8] derived the closed-form solutions for the deformation and fracture responses of a composite sandwich plate subjected to static indentation of a hemispherical-nose indenter. The composite sandwich plate was modeled as an infinite orthotropic elastic plate resting on a rigid-plastic foundation. They assumed that the face sheet deflection is several times the laminate thickness, so that the bending moments may be neglected and only the membrane forces are considered in the face sheet. They could also derive an approximate solution for the load–indentation response of the considered composite sandwich plates.

Hoo Fatt and Park [9] derived the approximate solutions for the static indentation and global deformation of sandwich panels. Then from these solutions, equivalent spring and dashpot forces were obtained. Equivalent masses, spring and dashpot were used in single and two degrees of freedom systems to find the low velocity impact response of the sandwich panel. Olsson and McManus [10] introduced an analytical model for the indentation of sandwich panels. They incorporated core crushing and large face sheet deflections in their model. The model was based on the assumption of axisymmetric indentation of an infinite elastic face sheet bonded to an elastic-ideally plastic core on a rigid foundation. Anderson and Madenci [11] investigated the force-indentation response of sandwich panels subjected to a rigid spherical indentor. The considered sandwich panels were made of graphite/epoxy face sheets with a polymethacrylimide foam core. They developed a three-dimensional analytical solution method to determine the complete stress and displacement fields in the sandwich panel, as well as the contact pressure arising from the static indentation by the rigid sphere.

In this paper, analytical solutions for the deformation response of a composite sandwich plate indented by a rigid flat-ended cylinder are derived using the principle of minimum potential energy. In contrast to the previous works, in derivation of the contact law (indentation force-indentation depth relation), a completely arbitrary staking sequence for the laminated face sheets as well as the initial in-plane forces acting on the edges of the sandwich plate are taken into consideration. Based on these modifications, an improved contact law is introduced. Low velocity impact analysis of the considered composite sandwich plate is analytically performed using a spring-mass-dashpot model that is established based on the derived contact law. Analytical predictions are compared with the experimental results published in the literature and the effects of some important parameters such as radius of the indenter, radius, mass and initial velocity of the impactor, ply thickness and stacking sequence of the face sheet and initial in-plane forces on load-indentation response and/or history of impact force of the sandwich plate are investigated and discussed.

2 FORMULATION OF THE PROBLEM

As shown in Fig. 1, a sandwich plate consisting of a honeycomb core and two laminated composite face sheets is considered. The face sheets are assumed to be completely elastic, while the core is elastic in tension and elastic-perfectly plastic in compression. Most Nomex and aluminum honeycombs and some foams show elastic-perfectly plastic behavior when they are subjected to transverse compressive loading [12]. The sandwich plate is rested on a rigid substrate and indented at the center of the top face sheet by a rigid, flat-ended cylinder of radius R. As shown in Fig. 1, ξ is the radius of deformation zone, δ the indentation depth, and q the crushing resistance of the honeycomb core.

It is assumed that the deformations of the top face sheet is several times of its thickness, so that the top face sheet can be considered as a membrane, i.e., its bending resistance is neglected. In the following two sections, the contact force – indentation relation (contact law) is derived first, and then it is used in the low velocity impact modeling of the problem, respectively.

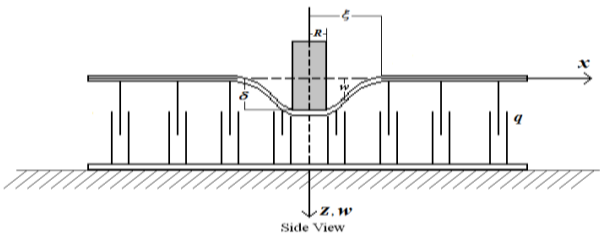

Fig. 1
A sandwich plate indented by a rigid, flat-ended cylinder.

2.1 Indentation analysis

The minimum total potential energy principle is utilized to derive the contact force - indentation relation. The total potential energy Π is [13]:

$$\Pi = U + D - W \tag{1}$$

where U is the elastic strain energy of the face sheet, D the plastic work dissipated in the crushing of the core and W the external work done. The indented surface of the face sheet w is assumed to be in the form of:

$$w(x,y) = \begin{cases} \delta & \text{for } 0 \le x^2 + y^2 \le R^2 \\ \delta\left[1 - \dfrac{(x-R)}{(\xi - R)}\right]^2 \left[1 - \dfrac{(y-R)}{(\xi - R)}\right]^2 & \text{for } R^2 \le x^2 + y^2 \le \xi^2,\ x \ge 0,\ y \ge 0 \end{cases} \tag{2}$$

The above function is assumed to be symmetric with respect to both x and y axis. Coefficients of the above function can satisfy the boundary conditions: zero slope and deflection at the boundary of the deformation zone.

The elastic strain energy U in the face sheet due to membrane forces is:

$$U = \frac{1}{2}\int_S N^T \varepsilon dS \tag{3}$$

where ε is the strain vector, N the in-plane force vector and dS the surface area. The nonlinear membrane strains are:

$$\varepsilon = \begin{pmatrix} \varepsilon_x^0 \\ \varepsilon_y^0 \\ \gamma_{xy}^0 \end{pmatrix} = \begin{pmatrix} \dfrac{1}{2}\left(\dfrac{\partial w}{\partial x}\right)^2 \\ \dfrac{1}{2}\left(\dfrac{\partial w}{\partial y}\right)^2 \\ \dfrac{\partial w}{\partial x}\dfrac{\partial w}{\partial y} \end{pmatrix} \tag{4}$$

Since, the in-plane deformations u and v are negligible in comparison with the transverse deflection w, so only the nonlinear terms are remained in Eq. (4). The analysis presented in this paper is nonlinear due to utilizing the nonlinear strain-displacement relations given by Eq. (4). The in-plane force vector N is:

$$N = \begin{pmatrix} N_x \\ N_y \\ N_{xy} \end{pmatrix} = \begin{bmatrix} A_{11} & A_{12} & A_{16} \\ A_{21} & A_{22} & A_{26} \\ A_{61} & A_{62} & A_{66} \end{bmatrix} \begin{pmatrix} \varepsilon_x^0 \\ \varepsilon_y^0 \\ \gamma_{xy}^0 \end{pmatrix} \tag{5}$$

where A_{ij} are the laminate extensional stiffnesses. Substituting Eqs. (4) and (5) into Eq. (3) gives:

$$U = \frac{1}{8}\int_S \left\{ A_{11}\left(\frac{\partial w}{\partial x}\right)^4 + A_{22}\left(\frac{\partial w}{\partial y}\right)^4 + 4A_{66}\left(\frac{\partial w}{\partial x}\right)^2\left(\frac{\partial w}{\partial y}\right)^2 + 2A_{12}\left(\frac{\partial w}{\partial x}\right)^2\left(\frac{\partial w}{\partial y}\right)^2 + 4A_{16}\left(\frac{\partial w}{\partial x}\right)^3\left(\frac{\partial w}{\partial y}\right) + 4A_{26}\left(\frac{\partial w}{\partial x}\right)\left(\frac{\partial w}{\partial y}\right)^3 \right\} dS \tag{6}$$

The integration area S in Eq. (6) consists of two regions: S_1, the area under the indenter which is a circle of radius R and S_2, the area outside the indenter which is a hollow circle of radii R and ξ (see Fig. 1). Since the indenter is flat-ended, across the region S_1, the derivatives $\frac{\partial w}{\partial x}$ and $\frac{\partial w}{\partial y}$ are zero and consequently, the integral over S_1 becomes zero. The integral over the region S_2, is approximated using the following assumption [8]:

$$\int_{S_2} dS = 4\int_{R}^{\xi}\int_{R}^{\xi} dxdy \tag{7}$$

Therefore, the elastic strain energy U becomes:

$$U = \frac{1}{2}\int_{R}^{\xi}\int_{R}^{\xi}\left\{A_{11}\left(\frac{\partial w}{\partial x}\right)^4 + A_{22}\left(\frac{\partial w}{\partial y}\right)^4 + 4A_{66}\left(\frac{\partial w}{\partial x}\right)^2\left(\frac{\partial w}{\partial y}\right)^2 + 2A_{12}\left(\frac{\partial w}{\partial x}\right)^2\left(\frac{\partial w}{\partial y}\right)^2 + 4A_{16}\left(\frac{\partial w}{\partial x}\right)^3\left(\frac{\partial w}{\partial y}\right) + 4A_{26}\left(\frac{\partial w}{\partial x}\right)\left(\frac{\partial w}{\partial y}\right)^3\right\} dxdy \tag{8}$$

Substituting derivatives of Eq. (2) into Eq. (8) gives:

$$U = \frac{\delta^4 E_1}{(R-\xi)^2} \tag{9}$$

where

$$E_1 = \left(\frac{8}{45}A_{11} + \frac{8}{45}A_{22} + \frac{32}{49}A_{66} + \frac{16}{49}A_{12} + \frac{2}{3}A_{16} + \frac{2}{3}A_{26}\right) \tag{10}$$

The plastic work dissipated in the crushing of the core is:

$$D = \pi q R^2 \delta + 4\int_{R}^{\xi}\int_{R}^{\xi} q w dxdy \tag{11}$$

where q is the crushing strength of the core. Using the profile given by Eq. (2), one gets:

$$D = \pi q R^2 \delta + \frac{4}{9} q \delta (R-\xi)^2 \tag{12}$$

The external work done W is [14]:

$$W = P\delta - \frac{1}{2}\int_{S}\left\{N_{xx}\left(\frac{\partial w}{\partial x}\right)^2 + N_{yy}\left(\frac{\partial w}{\partial y}\right)^2 + N_{xy}\frac{\partial w}{\partial x}\frac{\partial w}{\partial y}\right\} dS = P\delta - \frac{1}{30}\delta^2\left(16N_{xx} + 16N_{yy} + 15N_{xy}\right) \tag{13}$$

where P is the indentation force, N_{xx}, N_{yy} and N_{xy} are the initial in-plane forces acting on the edges of the sandwich plate and dS is the surface area. Therefore, the total potential energy is:

$$\Pi = \frac{\delta^4 E_1}{(R-\xi)^2} + \pi q R^2 \delta + \frac{4}{9} q \delta (R-\xi)^2 - P\delta + \frac{1}{30}\delta^2\left(16N_{xx} + 16N_{yy} + 15N_{xy}\right) \tag{14}$$

Minimizing Π with respect to δ gives:

$$P=\frac{4\delta^3 E_1}{(R-\xi)^2}+\pi qR^2+\frac{4}{9}q(R-\xi)^2+\frac{1}{15}\delta\left(16N_{xx}+16N_{yy}+15N_{xy}\right) \tag{15}$$

Similarly, minimizing P with respect to ξ gives:

$$\xi=\frac{0.0974\left(10^5\delta^3 E_1 q^3\right)^{1/4}}{q}+R \tag{16}$$

Substituting Eq. (16) into Eq. (15) gives the contact force - indentation relation (contact law) as:

$$\mathrm{P}=\frac{8\sqrt{E_1 q}\,\delta^{3/2}}{3}+\pi qR^2+\frac{1}{15}\delta\left(16N_{xx}+16N_{yy}+15N_{xy}\right) \tag{17}$$

2.2 Low velocity impact analysis

The contact force – indentation relation of the sandwich plate, Eq. (17), can be considered as the expressions for a nonlinear spring force and a constant force dashpot. For impact problem, the inertia of the impactor and deforming face sheet and core must be also taken into consideration. Low velocity impact problem of the sandwich plate can be approximated by a single-degree-of-freedom system consisting of the impactor mass M_0, the effective mass of the top face sheet m_f, a nonlinear spring and a constant force dashpot, as shown in Fig. 2. The inertia of the core is neglected compared to the face sheet and the impactor. The nonlinear spring in Fig. 2 has the following characteristics:

$$P_1(\delta)=\frac{8\sqrt{E_{1d}q_d}\,\delta^{3/2}}{3}+\frac{1}{15}\delta(16N_{xx}+16N_{yy}+15N_{xy}) \tag{18}$$

where E_{1d} is the dynamic membrane stiffness and q_d is the dynamic crushing strength of the core. The dynamic membrane stiffness E_{1d} has the same definition as the static membrane stiffness E_1, but it is obtained from a laminate membrane stiffness matrix that has been matched for high strain rate [9]. The dynamic crushing strength q_d is determined by tests. The constant force dashpot corresponds to the dynamic crushing strength of the core is characterized as:

$$Q_d=\pi q_d R^2 \tag{19}$$

It is assumed that the effective mass of the top face sheet is negligible, when compared to the mass of the impactor, $m_f \ll M_0$. Therefore, the local dynamic response can be described as:

$$M_0\ddot{\delta}+\mathrm{P}_1(\delta)+Q_d=0 \tag{20}$$

This is a nonlinear differential equation where the initial conditions are:

$$\dot{\delta}(0)=V_0 \tag{21}$$

$$\delta(0)=0 \tag{22}$$

This nonlinear differential equation can be solved numerically. The impact force is obtained as:

$$F(t)=-M_0\ddot{\delta}(t) \tag{23}$$

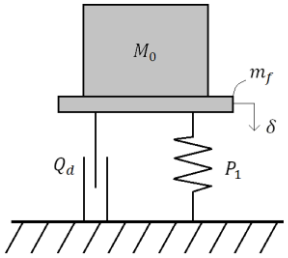

Fig. 2
Discrete modeling for low velocity impact of a rigidly supported sandwich plate.

3 COMPARISION WITH EXPERIMENTAL RESULTS

Williamson and Lagace [6] conducted some indentation and low velocity impact experiments on fully backed composite sandwich plates made with Nomex honeycomb core and AS4/3501-6 carbon/epoxy face sheet. The indenter and the impactor were hemispherical-nose cylinders made by case-hardened steel with the diameter of 25.4 *mm*. Material and geometrical properties of the sandwich plate as well as the impactor mass and the initial velocity are given in Table 1. To obtain both indentation and low velocity impact response of the sandwich plate, similar to [9], the hemispherical-nose cylinder was modeled as a flat-ended cylinder with an effective radius of $0.4R$. The experimental load-indentation curve for the composite sandwich plate obtained from the indentation experiments [6], is plotted in Fig. 3. In this figure, also the load-indentation response that is predicted by Eq. (17) is compared with the experimental result. As it is seen, the analytical predictions are in good agreement with the experimental results [6]. The analytical solution over-predicts the experimental data by acceptable discrepancy, because it was derived by the minimum total potential energy principle.

The experimental impact force-time curve for the composite sandwich plate obtained from low velocity impact experiments [6], is plotted in Fig. 4. Hoo Fatt and Park [9] showed that the dynamic membrane stiffness of woven carbon/epoxy laminate face sheet is almost equal to the static value. Therefore, it is assumed that:

$$E_{1d} = E_1 \tag{24}$$

At the other hand, the dynamic crushing strength of Nomex honeycomb is 10% greater than the static value [15], i.e.:

$$q_d = 1.1q \tag{25}$$

With the determined values of the parameters E_{1d} and q_d, the impact force-time response can be obtained from Eq. (23). The analytical result is compared with the experimental result [6] in Fig. 4. It is observed that the trends as well as the numerical values of the analytical predictions are in good agreement with those of the experimental results. However, the maximum impact force obtained by the present model is about 6% higher than that obtained from the experiment. This is due to the fact that the equivalent spring force was obtained from the static load-indentation response of the sandwich plate, which also over-predicted the experimental results as can be seen in Fig. 3.

4 PARAMETRIC STUDY

Now, the effects of some important parameters such as; radius of the indenter, radius, mass and initial velocity of the impactor, ply thickness and stacking sequence of the face sheet and initial in-plane forces on load-indentation response and/or history of impact force are studied. The material and geometrical properties of the considered sandwich plates are given in Table 1. The indenter/impactor is a flat-ended cylinder of radius 5.08 mm. Except for Figs. 9 and 10, the initial in-plane forces were considered to be zero in other Figures.

Table 1
Material and geometrical properties of the sandwich plate and the mass and the initial velocity of the impactor [6]

Face sheet	material: AS4/3501-6 carbon/epoxy $h = 0.175[mm]$ (ply thickness) stacking sequence:[0/90]	Core	material: Nomex honeycomb $H = 25.4\ [mm]$ (core thickness) $q = 1.389\ [MPa]$ (crushing resistance)
Ply stiffness	$E_{11} = 142\ [GPa]$ (longitudinal stiffness) $E_{22} = 9.8\ [GPa]$ (transverse stiffness) $G_{12} = 7.1[GPa]$ (in-plane shear modulus) $\nu_{12} = 0.3$ (Poisson's ratio)	Impactor	$M_0 = 1.61[kg]$ (mass) $V_0 = 1.2[m/s]$ (initial velocity)

4.1 Effect of ply thickness

The effect of ply thickness on load-indentation response and history of impact force is demonstrated in Figs. 5 and 6, respectively. As can be seen from Fig. 5, for the same indentation force, increasing the ply thickness causes the indentation to decrease. Additionally, sandwich plates with thicker face sheets have greater indentation force versus top face sheet deflection slope. Regarding the impact force history, as it is observed in Fig. 6, when the ply thickness is increased, the impact force increases, but the contact duration decreases. For instance, when the ply thickness is increased by 5 times, the maximum impact force is increased by 39% and the contact duration is decreased by 22%. These effects are likely due to the greater overall contact stiffness of the thicker face sheets.

4.2 Effect of stacking sequence

To study the effect of stacking sequence of the face sheet on the static indentation and the impact responses of the sandwich plate, the stacking sequence was considered as $[0/\theta/90/-\theta]$ and θ was varied as: $\theta = 15, 30, 45, 60, 75$. The results are shown in Figs. 7 and 8. As can be seen in these figures, the stacking sequence has a little influence on the static indentation as well as the impact responses. Identical results are observed for $\theta = 15$ and 75, and also for $\theta = 30$ and 60, for both static indentation and impact cases. Among the cases considered, the case $\theta = 45$ was found to be the most resistant one against the static indentation, since it gives the lowest indentation at a constant indentation force, and also the case with highest maximum impact force, while the cases $\theta = 15$ and 75 are on the contrary.

4.3 Effect of initial in-plane forces

In Figs. 9 and 10, the effect of initial in-plane forces on load-indentation response and history of impact force is illustrated, respectively. In view of these figures, it is observed that, if the case with zero initial in-plane forces be considered as a reference state, the positive initial in-plane forces decrease the indentation, increase the slope of the indentation force versus top face sheet deflection curve, increase the impact force and decrease the contact duration, while for the negative initial in-plane forces, these effects are exactly opposite. For instance, due to the existence of the initial in-plane forces $N_{xx} = N_{yy} = N_{xy} = 100\,\mathrm{kN/m}$, the maximum impact force is increased by 18% and the contact duration is decreased by 15%. The initial in-plane forces $N_{xx} = N_{yy} = N_{xy} = -100\,\mathrm{kN/m}$, conversely, cause the maximum impact force to decrease by 15% and the contact duration to increase by 25%.

4.4 Effect of radius of the indenter/impactor

The effect of radius of the indenter/impactor on load-indentation response and history of impact force is demonstrated in Figs. 11 and 12, respectively. As can be seen in Fig. 11, for the same indentation force, increasing the indenter radius, decreases the indentation. However, no change is observed in the slope of the indentation force versus top face sheet deflection curve, when the indenter radius increases. In the case of the impact force history, as it is seen in Fig. 12, by increasing the impactor radius, both the impact force and the contact duration decrease. For example, when the impactor radius is increased by 5 times, the impact force and the contact duration are decreased by 7% and 21%, respectively.

4.5 Effect of mass of the impactor

Fig. 13 shows the effect of mass of the impactor on the impact force history. It is observed that by increasing the mass of the impactor, both the impact force as well as the contact duration increase. As can be seen in Fig. 13, when the impactor mass is increased by 80%, the impact force and the contact duration are increased by 44% and 24%, respectively. However, the impact force history curves for different masses of the impactor, almost coincide in the first half period.

4.6 Effect of initial velocity of the impactor

In Fig. 14, the effect of initial velocity of the impactor on the impact force history is demonstrated. As can be seen in this figure, an increase in the initial velocity of the impactor, causes the impact force to increase, but it has almost no effect on the contact duration. For instance, an increase of 40% in the initial velocity of the impactor, causes 52% increase in the maximum impact force.

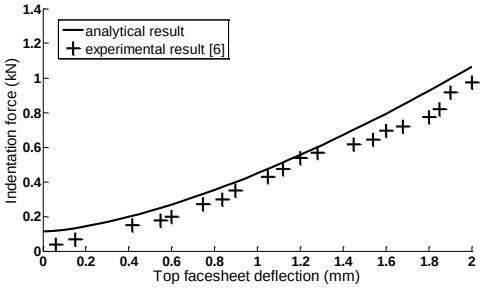

Fig. 3
Indentation force vs. top face sheet deflection for the composite sandwich plate.

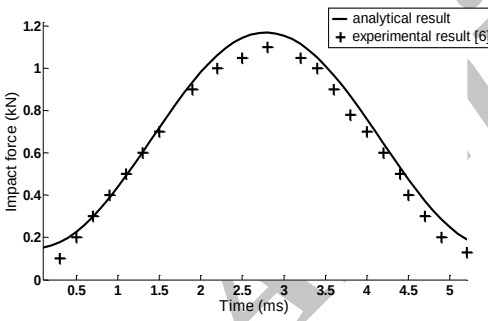

Fig. 4
Impact force vs. time for the composite sandwich plate.

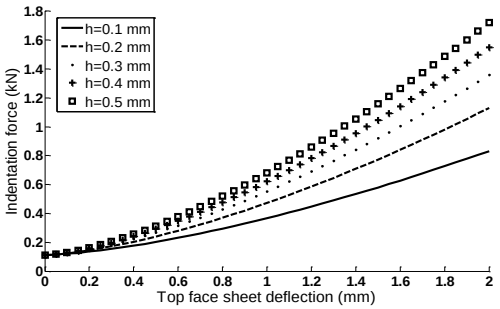

Fig. 5
Indentation force vs. top face sheet deflection for different ply thicknesses.

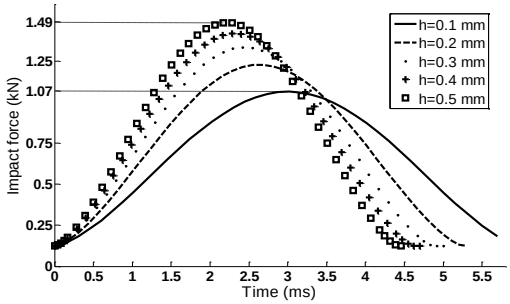

Fig. 6
Impact force vs. time for different ply thicknesses.

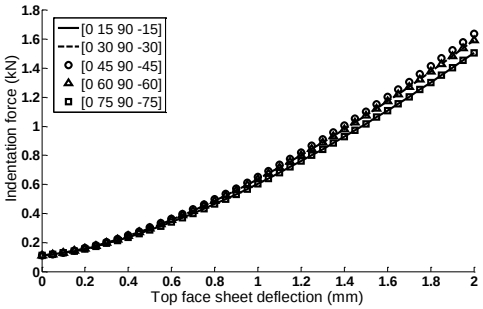

Fig. 7
Indentation force vs. top face sheet deflection for different stacking sequences of the face sheet.

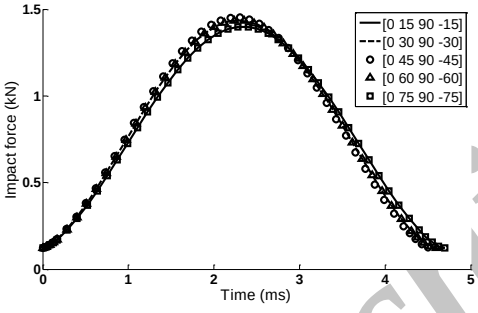

Fig.8
Impact force vs. time for different stacking sequences of the face sheet.

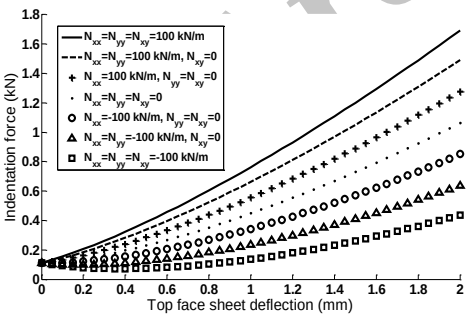

Fig. 9
Indentation force vs. top face sheet deflection for different initial in-plane forces.

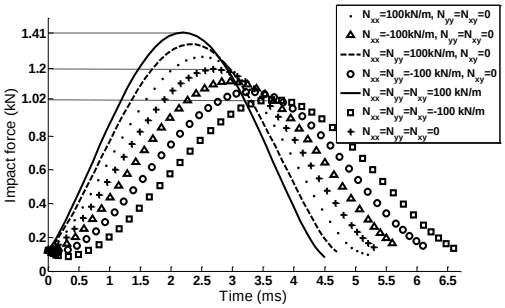

Fig. 10
Impact force vs. time for different initial in-plane forces.

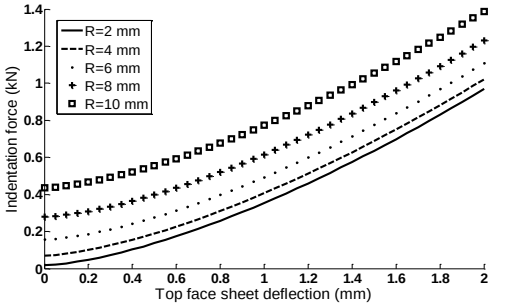

Fig. 11
Indentation force vs. top face sheet deflection for different values of the indenter radius.

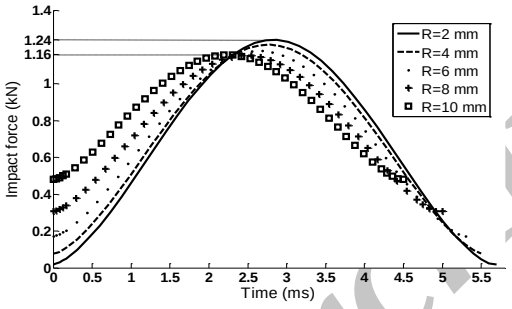

Fig. 12
Impact force vs. time for different values of the impactor radius.

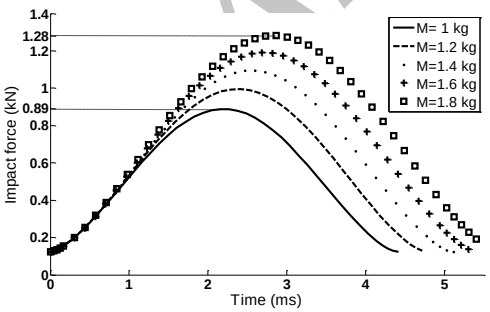

Fig. 13
Impact force vs. time for different values of impactor mass.

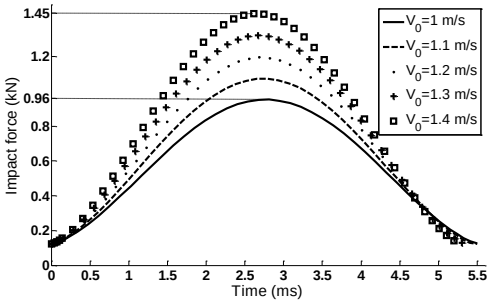

Fig. 14
Impact force vs. time for different values of the impactor initial velocity.

5 CONCLUSIONS

In this article, static indentation and low velocity impact responses of a fully backed composite sandwich plate subjected to a rigid flat-ended cylindrical indenter/impactor were analytically studied. In contrast to the previous works, the stacking sequence of the face sheets can be completely arbitrary. Moreover, the effects of the initial in-plane normal and shear forces acting on the edges of the sandwich plate are also considered. Based on these modifications, an improved contact law is introduced. Then, the low velocity impact analysis of the composite sandwich plates is performed using a spring-mass-dashpot model that is established based on the derived contact law. Considering the transverse flexibility of the structure and also the important engineering parameters, comprehensive analytical solutions are obtained for static indentation and low velocity impact responses of composite sandwich plates, which may be important tools for design engineers. The ease of use and the time saving advantages are achieved by the present analytical solutions. The validity of the present analysis is verified by experimental results. The effects of various parameters on both indentation and impact responses are studied. It is observed that the positive initial in-plane forces decrease the indentation and increase the impact force, while the negative initial in-plane forces, cause exactly the opposite effects. The stacking sequence of the face sheet has a little influence on the static indentation as well as the impact responses of the sandwich plate. Additionally, an increase in the initial velocity of the impactor has almost no effect on the contact duration.

REFERENCES

[1] Abrate S., 1998, *Impact on Composite Structures*, Cambridge University Press, Cambridge.
[2] Khalili M.R., 1992, Analysis of the dynamic response of large orthotropic elastic plates to transverse impact and its application to fiber reinforced plates, PhD thesis *, Indian Institute of Technology* , Delhi.
[3] Mittal R.K., Khalili M.R., 1994, Analysis of impact of a moving body on an orthotropic elastic plate, *The American Institute of Aeronautics and Astronautics* **32**(4):850-856.
[4] Wu H-YT., Chung F-K., 1989, Transient dynamic analysis of laminated composite plates subjected to transverse impact, *Computers & Structures* **31**:453-466.
[5] Gong S.W., Toh S.L., Shim P.W., 1994, The elastic response of orthotropic laminated cylindrical shells to low-velocity impact, *Composites Engineering* **4**(2):247-266.
[6] Williamson J.E., Lagace P.A., 1993, Response mechanism in the impact of graphite/epoxy honeycomb sandwich panels, *Proceeding of the Eighth ASC Technical Conference*, Cleveland, Ohio.
[7] Herup E.J., Palazotto A.N., 1997, Low-velocity impact damage initiation in graphite/epoxy/nomex honeycomb-sandwich plates, *Composites Science and Technology* **57**:1581-1598.
[8] Turk M.H., Hoo Fatt M.S., 1999, Localized damage response of composite sandwich plates, *Composites: Part B* **30**: 157-165.
[9] Hoo Fatt M.S., Park K.S., 2001, Dynamic models for low-velocity impact damage of composite sandwich panels- part a deformation, *Composite Structures* **52**:335-351.
[10] Olsson R., McManus H.L., 1996, Improved theory for contact indentation of sandwich panels, *The American Institute of Aeronautics and Astronautics* **34**:1238-1244.
[11] Anderson T., Madenci E., 2000, Graphite/epoxy foam sandwich panels under quasi-static indentation, *Engineering Fracture Mechanics* **67**:329-344.
[12] Gibson L.J., Ashby M.F., 1997, *Cellular Solids Structures and Properties*, Cambridge University Press, Cambridge.
[13] Malekzadeh K., Khalili M.R., Mittal R.K., 2006, Response of in-plane linearly prestressed composite sandwich panels with transversely flexible core to low-velocity impact, *Journal of Sandwich Structures and Materials* **8**:157-181.

[14] Hosseini M., Khalili S.M.R., Malekzadeh Fard K., 2011, Indentation analysis of in-plane prestressed composite sandwich plates: an improved contact law, *Proceedings of the Eighth International Conference on Composite Science and Technology*, Kuala Lumpur, Malaysia.

[15] Goldsmith W., Sackman J.L., 1991, An experimental study of energy absorption in impact on sandwich plates, *The International Journal of Impact Engineering* **12**(2):241-262.